Dependence of Calculated NMR Proton Chemical Shifts on Electron Density Properties in Proton-Transfer Processes on Short Strong Hydrogen Bonds

Luis F. Pacios*,† and Pedro C. Gómez‡

Unidad de Química, Departamento de Biotecnología, E.T.S. Ingenieros de Montes, Universidad Politécnica de Madrid, E-28040 Madrid, Spain, and Departamento de Química Física I, Facultad de Química, Universidad Complutense de Madrid, E-28040 Madrid, Spain

Received: July 26, 2004; In Final Form: October 6, 2004

Quantum chemical calculations were used to study the variation of NMR proton chemical shifts δ_H along the H-transfer process N−H···O → N···H···O → N···H−O in two short strong hydrogen bond (SSHB) systems: the anionic complex formed by 4-methylimidazole and acetate and the neutral complex formed by 4-methylimidazolium cation and acetate. Changes of δ_H associated with the H-transfer were studied at the equilibrium and one shorter N···O heteroatom distances in order to investigate the influence of stronger HB effects on chemical shifts. Optimized geometries and electron densities were obtained in MP2/6-311++G(*d*,*p*) calculations, while δ_H were computed at the B3LYP/6-311++G(*d*,*p*) level of theory. Extreme downfield shifts in the 15−20 ppm range for N−H···O and 13−18 ppm for N···H−O localized stages and maximum shifts about 23 ppm for the delocalized N···H···O state were found in agreement with data measured and computed before in SSHB systems as well as in biomolecular systems regarding enzymatic processes. These large chemical shifts that reveal extremely deshielded protons are shown to depend closely on local properties of the electron density, suggesting partially covalent features in the interaction underlying the SSHB environment.

Introduction

Short strong hydrogen bonds (SSHBs) have attracted a great deal of interest in the last years.[1−11] Any hydrogen bond A−H···B involves the sharing of H between the donor and acceptor partners to varying extents which in turn can be related to the A···B distance. Hydrogen is associated in most cases more with one heteroatom than the other; hence, the potential energy profile for the H-transfer process A−H···B → A···H−B must present two wells separated by a noticeable barrier. If the A···B distance is short enough, an A···H···B situation with nearly equal sharing of H between A and B could appear, the system should exhibit a single well, and the H-transfer process should be barrierless.[3] However, for certain A···B distances the energy profile can show two wells separated by a barrier so low that the central maximum can fall below the vibrational ground state, a situation referred to as low-barrier hydrogen bond (LBHB). The possible existence of LBHBs in the protected interiors of proteins and their significance for mechanisms of enzyme catalysis are still a matter of lively debate.[4−8] Although SSHB and LBHB are often used as nearly synonymous terms, they are not the same thing, as has been repeatedly pointed out.[7,9−11]

The evidence supplied by NMR spectroscopy is invaluable in probing hydrogen bonding characteristics[11−19] as far as the exposure of a delocalized proton decreases the electron density around the H nucleus, shifting the NMR signal to higher frequency (low field). On the basis of detailed studies on hydrogen bonding in organic compounds, Hibbert and Emsley[12] suggested that low-field proton chemical shifts (δ_H) in the 16−20 ppm range are consistent with SSHBs. This range encloses the unusually extreme low-field δ_H about 18 ppm formerly observed in proteases by Robillard and Schulman,[13] who assigned it to the $H^{\delta 1}$ atom of a histidine residue (see below), playing a central role in the catalytic activity of these enzymes for which the LBHB hypothesis was years after proposed.[5,14,15] The recent compilation by Mildvan et al.[14] of δ_H data measured for many complexes of enzymes and reaction intermediate or transition-state analogues for which high-resolution structures are available also reports a large set of highly deshielded proton resonances in the 15−20 ppm range. Very recently, a 15.41 ppm signal measured in the absence of inhibitor for the $H^{\delta 1}$ atom of His235 in hydroxynitrile lyase has been observed to shift to 19.35 ppm upon binding a strong inhibitor mimicking the transition state of a mechanism that implies the formation of a SSHB.[16] However, contrarily to what sometimes has been claimed,[5,15,17] such extreme low-field NMR chemical shifts are not conclusive evidence for LBHB but they just reveal largely deshielded protons. In fact, García-Viloca et al. for hydrogen maleate and hydrogen malonate[18] and Kumar and McAllister for several formic acid−formate and enol−enolate complexes[19] demonstrated theoretically that δ_H even greater than 22 ppm may appear in SSHBs without exhibiting a low-energy barrier to proton transfer. On the experimental side, a similar conclusion was also reported by Ash et al.[8] for *cis*-urocanic acid, a model system resembling the His-Asp diad present in the active site of proteases.

Insofar as unusual low-field shifts are characteristic of short HBs with sharings of H between both heteroatoms larger than that expected in conventional systems, the search for relationships between δ_H and HB strength parameters obtained in quantum calculations may help to establish the HB features

* Corresponding author. FAX: 34-91-3366387. E-mail: lpacios@montes.upm.es.
† Universidad Politécnica de Madrid.
‡ Universidad Complutense de Madrid.

10.1021/jp0466892 CCC: $27.50
Published on Web 12/04/2004

CHART 1

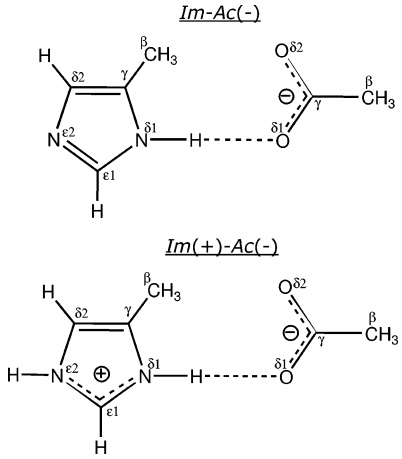

associated with NMR shifts greater than 15 ppm. In this regard, the information derived from the electron density $\rho(\mathbf{r})$ is especially relevant because strong deshielding is a direct consequence of electron redistribution around the H atom occurring upon hydrogen bonding. The conceptual framework provided by the theory of atoms in molecules (AIM) of Bader and collaborators[20,21] has proven invaluable in characterizing hydrogen bonding not only on theoretically computed densities but also on experimentally determined densities. We have recently started a research program[22−25] intended to study the variation with the intermolecular distance of AIM parameters and other molecular descriptors of the electron density and the electron localization function.[25] The reader can also find an updated account of the applications of AIM theory to hydrogen bonding in the introduction of refs 24 and 25.

In this work, we study SSHB complexes focusing on the changes of NMR proton chemical shifts accompanying the H-transfer from the donor to the acceptor in the systems formed by 4-methylimidazole and acetate and 4-methylimidazolium cation and acetate. These two complexes are chosen as SSHB models intended as reference to compare NMR shifts observed or computed for realistic systems in protein environments including His and Asp. The goals intended in the selection of these HB systems as well as the theoretical methodology used are presented in the following section. Our results are then reported and discussed, and finally the most relevant conclusions are summarized.

Systems Studied and Computational Methods

The HB systems studied are (a) the anionic complex formed by 4-methylimidazole and acetate, hereafter denoted Im and Ac(−), respectively, and (b) the neutral complex formed by 4-methylimidazolium cation, Im(+), and acetate, both depicted in Chart 1 where the atom labeling similar to that used for amino acids in proteins is also introduced. Whereas Im−Ac(−) represents a model for unprotonated histidine and aspartate side chains, Im(+)−Ac(−) is the analogous model for that pair upon protonation of imidazole ring, with β methyl groups substituting the linking to backbone peptide chain in both cases. We study here the proton transfer from the $N^{\delta1}$ donor atom of Im and Im(+) to the $O^{\delta1}$ acceptor atom of Ac(−) at two different $N^{\delta1}\cdots O^{\delta1}$ distances in every complex selected as explained below.

While the general mechanism of peptide hydrolysis is a known topic covered in most biochemistry textbooks, the molecular details are still under investigation. The role played by the HB between $N^{\delta1}$ of histidine and $O^{\delta1}$ of asparte in active sites of serine proteases is interesting not only for enzymatic processes but also for hydrogen bonding research. Side chains of His-Asp diads present an arrangement like Im−Ac(−) in free enzymes, whereas binding the substrate occurs upon protonation of imidazole as in Im(+)−Ac(−). However, the systems in Chart 1 neither intend to mimick those active sites nor the H-transfer studied here really occurs in those mechanisms because protonation of aspartate is avoided by water molecules and other side chains in the vicinity of carboxylate (see for instance ref 27). Our goal in computing the changes of NMR chemical shifts associated with the proton transfer in these SSHB systems is 2-fold. On one side is exploration of HB features associated with extreme low-field chemical shifts. On the other side is providing reference results for comparisons intended to estimate local protein environmental effects underlying δ_H data either measured or computed for realistic models of enzyme/substrate complexes with other theoretical approaches.[14,17,26−28]

Since electron correlation is a leading effect in hydrogen bonding, correlated calculations are absolutely mandatory. We resorted to the MP2 approach, a reliable workhorse for including correlation in molecular systems of medium size, to obtain geometries, energies, and electron densities. The basis set selected was 6-311++G(*d*,*p*), a fair compromise between flexibility and affordable size as its ability to predict accurate geometries and energies has before demonstrated.[23−25,29] Geometries were thus optimized in ab initio MP2/6-311++G(*d*,*p*) calculations as follows. Isolated 4-methylimidazole and acetate monomers were first optimized without constraints and then reoptimized upon forcing C_{3v} symmetry in methyls. This constraint yields negligible differences in structures and energies; hence, considering the large number of optimizations needed, we froze the internal geometry of methyls, although torsion angles with imidazole and carboxylate were optimized in all cases. With this only constraint, an $N^{\delta1}\cdots O^{\delta1}$ distance of 2.647 Å and $N^{\delta1}H$ bond length of 1.069 Å for Im−Ac(−) and an $N^{\delta1}\cdots O^{\delta1}$ distance of 2.751 Å for Im(+)−Ac(−) were found. The optimization predicts for this last system complete proton transfer to the $O^{\delta1}$ atom of acetate with an OH length of 0.998 Å (the $N^{\delta1}\cdots H$ distance is 1.763 Å), the dimer becoming now that formed by neutral Im (with an $N^{\epsilon2}H$ bond) and acetic acid. To study the H-transfer, we optimized then geometries for fixed $N^{\delta1}H$ bond lengths ranging from 1.0 to 1.8 Å at fixed $N^{\delta1}\cdots O^{\delta1}$ distances of 2.65 Å in Im−*Ac*(−) and 2.75 Å in Im(+)−Ac(−).

To assess the effect of closer proximity between monomers on the computed δ_H, we studied the H-transfer at a fixed $N^{\delta1}\cdots O^{\delta1}$ distance of 2.55 Å in both complexes, optimizing equivalent sets of geometries at fixed $N^{\delta1}H$ bond lengths as done at equilibrium heteroatom separations. In the recent compilation of NMR data by Mildvan et al.,[14] N···O distances ranging from 2.45 to 2.65 Å are reported for several enzymes with His-Asp or His-Glu diads in their active sites. The selected 2.55 Å length is thus a representative value of this range and, being equal for both Im−Ac(−) and Im(+)−Ac(−), allows for testing the effect of protonating imidazole on the SSHB characteristics underlying the changes of δ_H in the H-transfer. The criterion to set the particular $N^{\delta1}H$ lengths considered and thus the number of optimizations for every system was to trace out properly the potential energy profiles (see below). This resulted in 11 geometries for $N^{\delta1}\cdots O^{\delta1}$ distances of 2.65 and 2.55 Å in Im−Ac(−) and 11 for 2.55 and 15 for 2.75 Å in Im(+)−Ac(−), which makes a total of 48 MP2/6-311++G(*d*,*p*) geometries. Although some features of these potential curves relevant for the subsequent discussion are briefly mentioned

below, the geometries and energy profiles as well as environment effects originated by media of low polarity (like protein interiors) and high polarity (like water) are analyzed in depth in a separate paper.[30]

Electron densities were then obtained in separate single-point MP2/6-311++G(*d*,*p*) calculations at every geometry and the critical points of $\rho(\mathbf{r})$ located and characterized using EXTREME.[31] NMR shielding tensors were determined through the GIAO (gauge invariant atomic orbital) approach[32] and the chemical shifts calculated with respect to tetramethylsilane (TMS). Because gas phase is implied in theoretical calculations, we pursued also to estimate the effect on δ_H of media of variable polarity like those surrounding SSHBs in active sites of proteins.[33,34] The only method to include solvent effects on GIAO calculations is currently the polarizable continuum model (PCM).[35] We performed exploratory GIAO−PCM calculations in water and chloroform to simulate media of distinct polarity at some selected geometries. As far as this approach is concerned, the differences between both solvents were found negligible (results not shown); hence, the additional GIAO−PCM calculations were finally done in chloroform not only because it is a solvent often used for NMR measurements but also because its dielectric constant ($\epsilon = 4.9$) is representative of protein interiors.[33] However, the costly computational demands posed by GIAO MP2 calculations and the need to compute two values of δ_H (gas phase and chloroform) at every one of the 48 geometries considered forced us to select the less demanding B3LYP approach to include correlation in δ_H. This method is known to give results of accuracy comparable to MP2 for HB systems;[23,24,29] therefore, after some calculations in the monomers to gauge the reliability of B3LYP instead MP2 chemical shifts (see below), the δ_H reported in this paper for the complexes are B3LYP results. To discuss the importance of correlation effects on chemical shifts, Hartree−Fock (HF) GIAO calculations were also carried out. All these HF, MP2 (in monomers), B3LYP (gas), and B3LYP (PCM, chloroform) GIAO calculations were accomplished with the 6-311++G(*d*,*p*) basis set at MP2 geometries. The same computational scheme was applied to TMS for which the MP2/6-311++G(*d*,*p*) geometry was previously optimized. All these calculations were done with GAUSSIAN98[36] and GAUSSIAN03.[37]

Results and Discussion

Energy profiles for the proton transfer including environment effects in the SSHB systems in Chart 1 have been discussed separately;[30] hence, we report here only on some features intended to provide an energetic picture before discussing the properties addressed below. These MP2/6-311++G(*d*,*p*) energy profiles are plotted in Figures 1 and 2 at the intermolecular $N^{\delta1}\cdots O^{\delta1}$ distances (denoted *R*(NO) hereafter) presented in the preceding section. Environment effects[30] were accounted for by means of isodensity PCM (IPCM)[38] calculations: this approach uses isodensity contours of the $\rho(\mathbf{r})$ iteratively computed under the effect of a polarizable continuum to set the cavity shape (for the performance of IPCM, see also ref 39). Gas-phase ($\epsilon = 1$) as well as $\epsilon = 5$ (chloroform) and $\epsilon = 78.39$ (water) results are shown in Figures 1 and 2. Two separate wells are seen in the gas phase only in Im−Ac(−) at equilibrium *R*(NO) = 2.65 Å, while protonation of acetate yields no longer a stable state with respect to intermediate R_{NH} values at 2.55 Å. For Im(+)−Ac(−), H-transfer to acetate is a downhill process rendering a single well for acetic acid, although a small plateau at 2.75 Å when H is still near Im(+) is seen. At this point, Im−Ac(−) at its equilibrium *R*(NO) is the only system showing a barrier to the proton transfer in the gas phase with a height of 6.7 kcal/mol with respect to the deepest well and a separation between minima of 6.1 kcal/mol [30] (no vibrational states were considered at this stage).

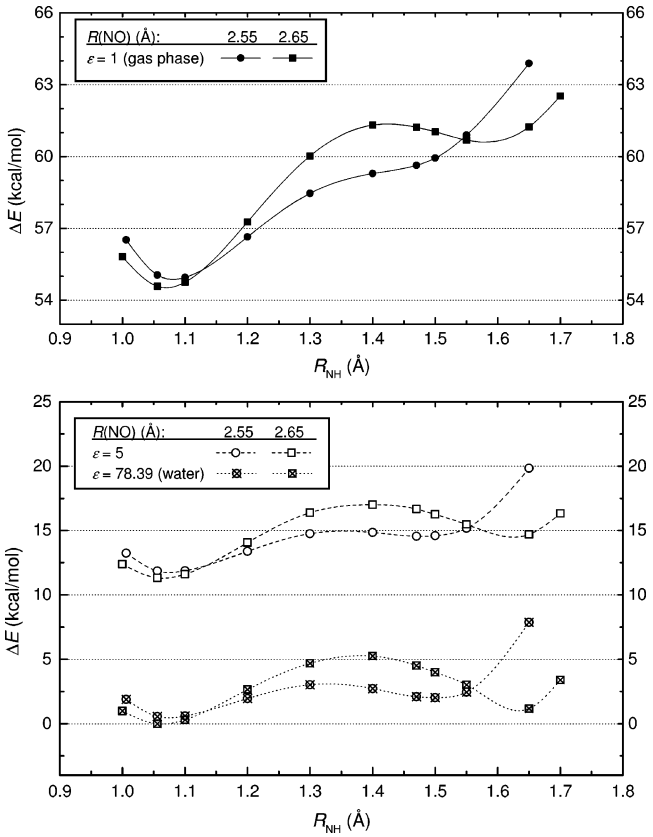

Figure 1. MP2/6-311++G(*d*,*p*) energy profiles for the proton transfer in Im−Ac(−) at intermolecular $N^{\delta1}\cdots O^{\delta1}$ distances *R*(NO) = 2.55 and 2.65 Å (equilibrium). Top panel: gas-phase results. Bottom panel: environment effects obtained in IPCM calculations for $\epsilon = 5$ and $\epsilon = 78.39$ (water). R_{NH} is the $N^{\delta1}$−H distance (the origin of the Δ*E* scale in both panels is the same).

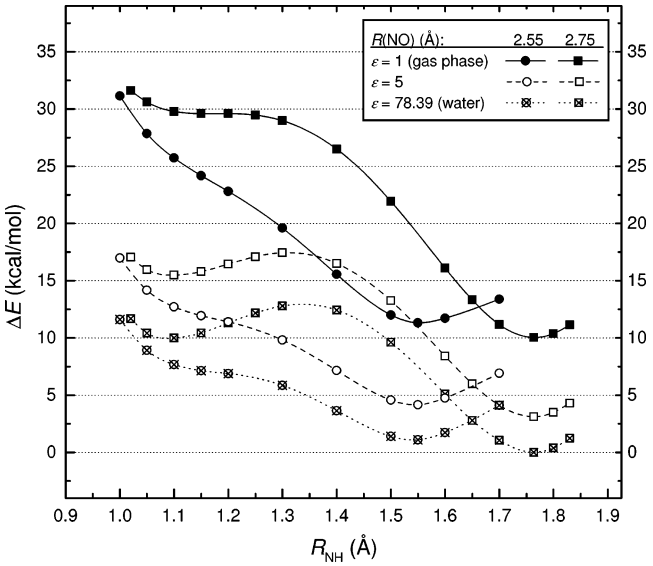

Figure 2. MP2/6-311++G(*d*,*p*) energy profiles for the proton transfer in Im(+)−Ac(−) at intermolecular $N^{\delta1}\cdots O^{\delta1}$ distances *R*(NO) = 2.55 and 2.75 Å (equilibrium). Environment effects obtained in IPCM calculations for $\epsilon = 5$ and $\epsilon = 78.39$ (water). R_{NH} is the $N^{\delta1}$−H distance.

Environment effects modify this picture, giving rise to two minima except for Im(+)−Ac(−) at *R*(NO) = 2.55 Å. Curves

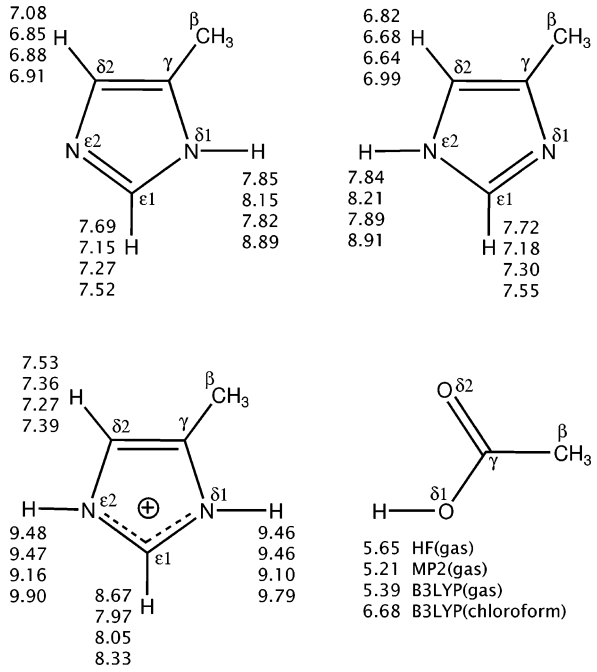

Figure 3. Proton NMR chemical shifts δ_H for neutral 4-methylimidazole with the H atom at $N^{\delta 1}$ and $N^{\epsilon 2}$ locations (upper row) and 4-methylimidazolium cation and acetic acid (lower row) computed with the 6-311++G(*d*,*p*) basis set. The sequence of methods to calculate the set of δ_H values listed for every hydrogen corresponds to that indicated for acetic acid.

for Im−Ac(−) show nearly identical shape under the two media and similar energy differences between wells at both N···O distances: 2.7 kcal/mol at *R*(NO) = 2.55 Å and 3.4 kcal/mol at 2.65 Å for $\epsilon = 5$, and 1.5 and 1.2 kcal/mol, respectively, for water. The corresponding barrier heights are, however, different: 3.0 and 5.7 kcal/mol at 2.55 and 2.65 Å for $\epsilon = 5$, and 2.5 and 5.2 kcal/mol for water. Relative to the gas phase, polar media stabilize protonation of acetate with water, yielding nearly symmetrical energy curves. On the other side, the barrier is decreased at the shorter *R*(NO) by an equal magnitude under both media, 2.7 kcal/mol, which is the difference between 2.55 and 2.65 Å results. Neutral Im(+)−Ac(−) only exhibits two wells at its equilibrium *R*(NO) with energy differences between minima of 12.4 ($\epsilon = 5$) and 10.0 kcal/mol (water) and barrier heights with respect to the left minimum of 1.9 ($\epsilon = 5$) and 2.8 kcal/mol (water). At the shorter *R*(NO), the only distinct feature is the smaller slope at the left side of the curves, especially in water. Contrarily to what happens for the ionic complex, polar media stabilize the protonated imidazole ring relative to gas phase, although the barrier to the strongly stabilized H-transfer to acetate is rather small. A common characteristic noticed in all cases is the overall lower energies in water, an issue recently highlighted for ionic HBs.[7c]

Before discussing changes of δ_H accompanying the proton transfer, we compare in Figure 3 results obtained at different levels of theory for the monomers involved. HF results deviate noticeably from correlated MP2 or B3LYP values only at $C^{\epsilon 1}$ in imidazole and at hydroxyl in acetic acid, whereas the rest of the hydrogens show small differences. As for the solvent effect, chloroform shifs the δ_H signal to lower field values in all cases with greater increases for more deshielded protons linked to electronegative N and O atoms. The distinct magnitude of δ_H for imidazole protons is consistently reproduced by all the methods and agrees reasonably with reported data. For instance, $\delta_H = 7.14$ for H at $C^{\delta 2}$ and 8.12 ppm for $C^{\epsilon 1}$ were measured for histidine in the random coil conformation of the tetrapeptide Gly-Gly-His-Ala,[40] while 6.99 and 8.10 ppm were reported for the same atoms from NMR measurements in proteins[41] (ring N protons are not usually observed). On the theoretical side, two recent reports providing reliable NMR data on models of the catalytic site of chymotrypsin are worth mentioning: the density functional theory (DFT) quantum calculations including vibrational averages and calibration corrections by Westler et al.[26] and the combined QM(HF)/MM and ONIOM-NMR study of Molina and Jensen[27] (we shall refer again to these reports when discussing the variation of δ_H). Some side results on monomers were included in these works and are relevant here: $\delta_H = 8.6$ for $C^{\epsilon 1}$ and 9.4 ppm for $N^{\delta 1}$ in Im(+) reported by Molina and Jensen and $\delta_H = 5.45$ ppm for monomeric acetic acid given by Westler et al. (the predominant species in liquid acetic acid is the dimer as the measured 11.65 ppm value agrees closely with the 11.8 ppm result obtained by these authors for dimeric acetic acid). It should be also noted that neutral Im monomers show shifts virtually indistinguishable for H at $N^{\delta 1}$ or $N^{\epsilon 2}$, while in protonated imidazole both hydrogens exhibit largely increased δ_H values, about 9 ppm in the gas phase and near 10 ppm in chloroform.

Whereas correlation effects on computed NMR shifts are usually considered important for heavy atoms but relatively small (about 0.1−0.3 ppm) for hydrogens,[42] their influence is known to increase in strong HBs.[43] In fact, gas-phase values in Figure 3 show that correlation decreases δ_H by about 0.1−0.3 ppm in all protons except those at $C^{\epsilon 1}$ for which correlated values are 0.4−0.7 ppm smaller. However, the complexes show a rather different behavior. Figure 4 plots the variation of δ_H for the proton transferred from $N^{\delta 1}$ to $O^{\delta 1}$ in Im−Ac(−) and Im(+)−Ac(−) at their equilibrium *R*(NO) distances. While uncorrelated and correlated results are reasonably similar at both ends of the curves (that involve $N^{\delta 1}$−H···$O^{\delta 1}$ and $N^{\delta 1}$···H−$O^{\delta 1}$ localized states), HF results deviate noticeably and reach δ_H peak values about 25 ppm at intermediate R_{NH} lengths (that involve delocalized $N^{\delta 1}$···H···$O^{\delta 1}$ states). This greater effect of correlation on most deshielded protons must be analyzed in light of the features exhibited by $\rho(\mathbf{r})$ (see the discussion below). Since the influence of electron correlation on NMR chemical shifts increases with HB strength,[18,26,43] uncorrelated calculations to obtain δ_H in SSHB systems should be avoided if the study focuses on H-transfer. In fact, at R_{NH} distances for which H is nearly equidistant from heteroatoms, the system $N^{\delta 1}$···H···$O^{\delta 1}$ can be viewed as linked by two HBs with both monomers playing simultaneously donor and acceptor roles; hence, correlation effects reach their largest extent. In this regard, it is illustrative to contrast Figure 4 with published data. Chemical shift distributions across B3LYP/6-311++G(2*d*,2*p*) potential curves for hydrogen maleate and hydrogen 2,2-dimethylmalonate (symmetrical O···H···O strong HB systems) reported by Westler et al. show δ_H peak values of about 22.5 ppm (see Figure 2 in ref 26). Molina and Jensen studied proton transfer from histidine to aspartate in a subsystem of chymotrypsin corresponding to the protein environment within 7 Å of the active site. These authors plot the variation of δ_H obtained from HF calculations with the $N^{\delta 1}$−H distance, finding peak values about 25 ppm for intermediate $N^{\delta 1}$···H···$O^{\delta 1}$ proton location (see Figure 6 in ref 27b). Although the complexes dealt with here are different, note how peak values a bit greater than 22 ppm for correlated B3LYP and about 25 ppm for uncorrelated HF results are also seen in Figure 4. This concordance should suggest similar deshielding when the proton locates far from both heteroatoms, regardless of the particular nature of donor and acceptor partners in the SSHB system. On the other side,

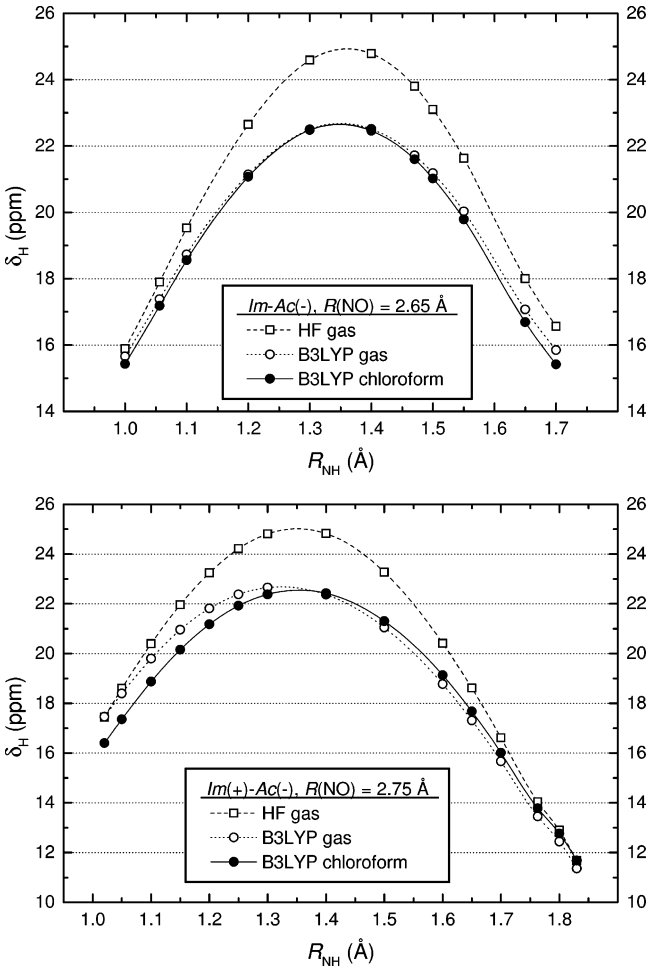

Figure 4. Variation of NMR chemical shifts with the $N^{\delta1}$−H distance obtained by the GIAO method in uncorrelated HF and correlated B3LYP calculations with the 6-311++G(*d*,*p*) basis set for the H atom transferred from $N^{\delta1}$ to $O^{\delta1}$ in Im−Ac(−) (top panel) and Im(+)−Ac(−) (bottom panel) at their equilibrium $N^{\delta1}\cdots O^{\delta1}$ distances.

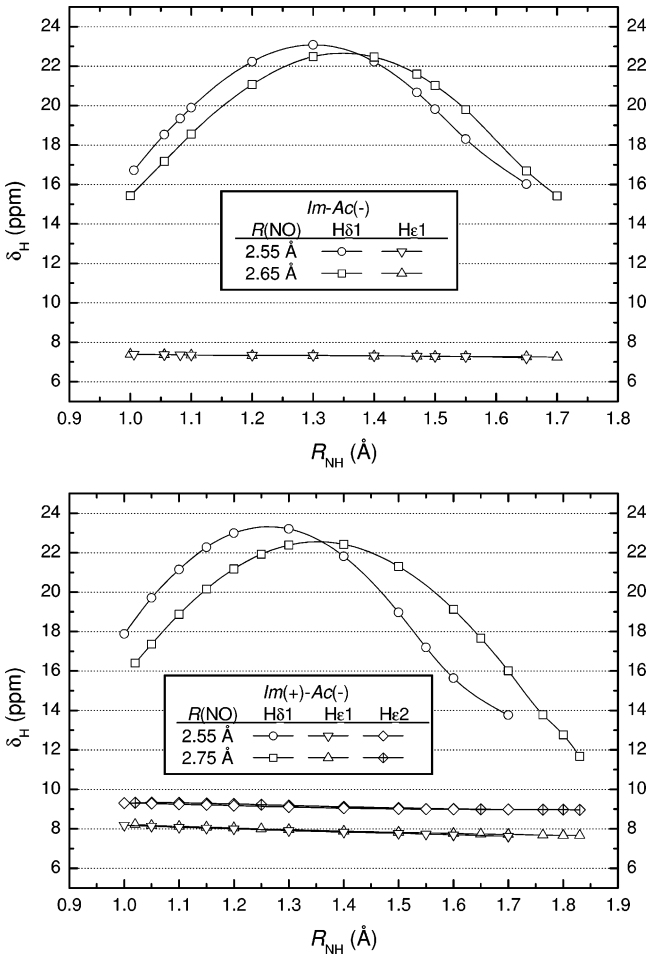

Figure 5. Variation of B3LYP(chloroform)/6-311++G(*d*,*p*) NMR chemical shifts with the $N^{\delta1}$−H distance for H atoms at $N^{\delta1}$ and $C^{\epsilon1}$ locations in Im−Ac(−) at *R*(NO) = 2.55 and 2.65 Å (top panel) and for H atoms at $N^{\delta1}$, $C^{\epsilon1}$, and $N^{\epsilon2}$ locations in Im(+)−Ac(−) at *R*(NO) = 2.55 and 2.75 Å (bottom panel).

solvent appears to have vey little effect on chemical shifts. Only at short R_{NH} distances in Im(+)−Ac(−) both B3LYP δ_H values differ about 1 ppm, the difference falls then to about 0.5 ppm at R_{NH} = 1.2 Å, and chloroform and gas-phase curves become finally nearly indistinguishable at longer distances.

Figure 5 shows the variation of B3LYP chemical shifts of the following protons: (i) that transferred from $N^{\delta1}$ to $O^{\delta1}$, (ii) that bonded at $C^{\epsilon1}$ in both complexes, and (iii) that bonded to $N^{\epsilon2}$ in Im(+), while Table 1 gathers some selected data helpful in analyzing this variation. The curves of $H^{\delta1}$ in the top panel of Figure 5 exhibit similar values at R_{NH} in the proximity of either $N^{\delta1}$ and $O^{\delta1}$ atoms regardless of the relative stability of the underlying transfer stages seen in Figure 1, which indeed suggests similar deshielding for $N^{\delta1}$−H$\cdots O^{\delta1}$ and $N^{\delta1}\cdots$H−$O^{\delta1}$ states in Im−Ac(−). On the contrary, the transfer to yield acetic acid in Im(+)−Ac(−) gives rise to much smaller chemical shifts at the $N^{\delta1}\cdots$H−$O^{\delta1}$ domain: see how δ_H falls below 15 ppm before completing the transfer in the bottom panel of Figure 5. Save for this difference, both complexes behave rather similarly at their intermolecular equilibrium distances. At the closer *R*(NO) = 2.55 Å separation, protonating imidazole shifts downfield the NMR signal of $H^{\delta1}$ when it is still near $N^{\delta1}$: compare δ_H at R_{NH} below 1.30 Å for both complexes at 2.55 Å in Table 1. As seen in Figure 3, this effect is already noticed in the monomers. In fact, the electron redistribution involved in bonding the extra proton in Im(+) deshields the three hydrogens

TABLE 1: Values of B3LYP NMR Chemical Shifts δ_H for the Proton Transferred between $N^{\delta1}$ and $O^{\delta1}$ Atoms at Selected Intervals of R_{NH} Distances in the Complexes Displayed in Chart 1 (R_{NH} in Å, δ_H in ppm)

	R(NO) = 2.55 Å	equilibrium *R*(NO)[a]
Im−Ac(−)		
local minimum energy at R_{NH} =[b]	1.07	1.07, 1.60
δ_H at interval R_{NH} = 1.05−1.10	18.5−19.9	17.2−18.6
δ_H at interval R_{NH} = 1.10−1.30	19.9−23.1	18.6−22.5
δ_H at interval R_{NH} = 1.55−1.65	18.3−16.0	19.8−16.7
maximum δ_H (at R_{NH})	23.1 (1.30)	22.6 (1.35)
Im(+)−Ac(−)		
local minimum energy at R_{NH} =[b]	1.55	1.76
δ_H at interval R_{NH} = 1.05−1.10	19.7−21.2	17.4−18.9
δ_H at interval R_{NH} = 1.10−1.30	21.2−23.2	18.9−22.4
δ_H at interval R_{NH} = 1.55−1.75	17.2−13.8	19.1−13.8
maximum δ_H (at R_{NH})	23.2 (1.30)	22.5 (1.35)

[a] 2.65 Å in Im−Ac(−), 2.75 Å in Im(+)−Ac(−). [b] See Figures 1 and 2.

in the $N^{\epsilon2}$−$C^{\epsilon1}$−$N^{\delta1}$ moiety, increasing their δ_H values with respect to their corresponding values in neutral imidazole. However, as data collected in Table 1 illustrate, this shift is amplified by the short HB effect, whereas, at equilibrium *R*(NO) distances, it amounts to only 0.2−0.3 ppm (compare δ_H at R_{NH} = 1.05−1.10 intervals). On the other side, peak values are virtually identical for both complexes, suggesting essentially indistinguishable delocalized $N^{\delta1}\cdots$H$\cdots O^{\delta1}$ states, although

again the shorter HB distance at 2.55 Å increases peak δ_H by about 0.5 ppm. It should be then stressed that, despite the differences in the relative stability of H-transfer stages arising from protonating imidazole, both complexes show similar deshielding effects on the H transferred and consequently similar sensitivity to heteroatom distance.

Regarding the rest of protons, $H^{\epsilon 1}$ changes along the whole range of R_{NH} only from 7.4 to 7.2 ppm in Im−Ac(−), while $H^{\epsilon 2}$ does from 9.3 to 9.0 ppm in Im(+)−Ac(−), values in both cases smaller than their 7.5 and 9.9 ppm monomer counterparts, respectively (see Figure 3). However, $H^{\epsilon 1}$ in Im(+)−Ac(−) changes from 8.2 to 7.7 ppm, a little greater variation that conveys an interesting information. In fact, upon protonating imidazole, $H^{\epsilon 1}$ feels in Im(+) the electron redistribution conventionally depicted as in Chart 1 to represent two equivalent resonance structures in the $N^{\epsilon 2}-C^{\epsilon 1}-N^{\delta 1}$ moiety. When the H being transferred is still near $N^{\delta 1}$ in Im(+)−Ac(−), the δ_H of $H^{\epsilon 1}$ is 8.2 ppm, a result close to the value in the Im(+) monomer, 8.3 ppm. As $H^{\delta 1}$ moves farther from imidazole, the resonance effect implied in its bond weakens and $H^{\epsilon 1}$ behaves like that in neutral Im. At long R_{NH} distances where $H^{\delta 1}$ has been already transferred and neutral imidazole with H at $N^{\epsilon 2}$ is left behind, the δ_H of $H^{\epsilon 1}$ is 7.7 ppm, still larger than the monomer 7.55 ppm value. If one considers that the other protons have chemical shifts smaller in the complexes than in the monomers, this result suggests that $H^{\epsilon 1}$ could still feel a residual electron resonance effect in Im(+)−Ac(−) even at the localized $N^{\delta 1}\cdots H-O^{\delta 1}$ state. In any event, the behavior of these shifts illustrates the importance of local electron density effects responsible for NMR deshielding associated with hydrogen bonding. It is not an infrequent finding in the literature discussions on biomolecules that seem to imply that HBs should be explained in purely electrostatic terms. Not only the way this topic is covered in most biochemistry textbooks but also many arguments stated in favor of[5] or against[7] the LBHB hypothesis in reports on enzymes illustrate the point. If a major conclusion is drawn from research in past years, it is that quantum effects associated with local redistributions of electron density play an essential role in the interactions underlying any type of hydrogen bonding (see for instance refs 23 and 24 and references therein).

Since the complexes studied represent bare reference systems for quantifying SSHB effects on δ_H, the comparison of our results with some data of enzymes in which the interaction between histidine and aspartate is instrumental in explaining catalytic activity may cast some light on the extent to which HB effects account for the large magnitude of NMR shifts. Measured values of 18.2 ppm [44] in chymotrypsin and 17.1 [45] in α-lytic protease have been recently published for $H^{\delta 1}$ in His. A shift of 18.2 ppm [46] has been also observed in chymotrypsinogen and signals varying between 18.61 and 18.95 ppm [47] reported for complexes of chymotrypsin and four peptidyl trifluoro methyl ketones (TFKs), which are analogues of tetrahedral intermediates formed during the catalytic activity. In this case, $H^{\delta 1}$ becomes increasingly deshielded with increasing affinity of peptidyl TFKs for the enzyme; that is, δ_H rises with the expected greater strength of the HB formed.[17] In the compilation by Mildvan et al.,[14] chemical shifts between 17.4 and 18.9 ppm are reported for serine proteases (His interacting with Asp) and between 15.5 and 18.1 ppm for serine esterases (His interacting with Glu). All these data involve enzyme/substrate complexes, and therefore His is protonated. For the ranges of R(NO) and R_{NH} implied in these examples, our δ_H results for Im(+)−Ac(−) are between 18 and 21 ppm, with larger shifts belonging to shorter R(NO) distances. On the theoretical side, the highly

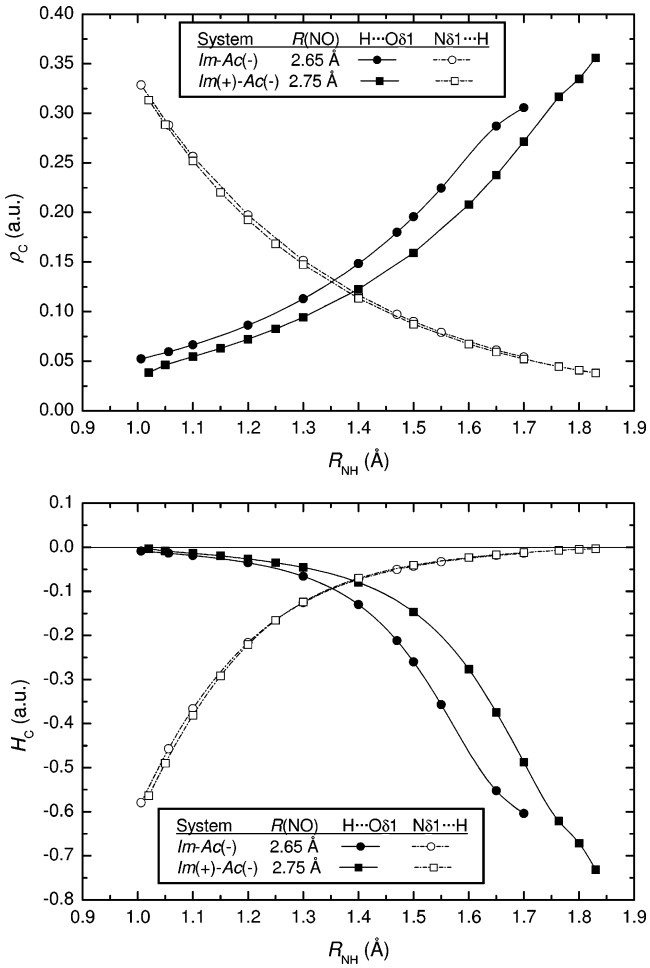

Figure 6. Variation with the $N^{\delta 1}-H$ distance of local values of the electron density, ρ_C (top panel), and total energy density, H_C (bottom panel), computed at bond critical points in $H\cdots O^{\delta 1}$ and $N^{\delta 1}\cdots H$ paths with the MP2/6-311++G(*d*,*p*) electron density in Im−Ac(−) and Im(+)−Ac(−) at their R(NO) equilibrium distances 2.65 and 2.75 Å, respectively.

accurate correlated results including vibrational averages of Westler et al.[26] on realistic structural models of the catalytic site of chymotrypsin predict 17.7 ppm for $H^{\delta 1}$ of His when R(NO) is 2.75 Å and 21.4 ppm at 2.55 Å (see Table 2 and Figure 6 in ref 26): our results for equivalent R_{NH} lengths are 18.2 and 20.5 ppm, respectively. These authors also report measured data for the other protons in imidazole, but since $H^{\epsilon 1}$ and $H^{\epsilon 2}$ participate in HBs formed between histidine and other residues, they show δ_H = 9.25 and 13.2 ppm, respectively.[26] If one compares our equivalent results for $H^{\epsilon 1}$ and $H^{\epsilon 2}$, 8.2 and 9.3 ppm, respectively, in Im(+)−Ac(−), the differences found are consistent with the relative strength of these HBs. In fact, $H^{\epsilon 1}$ makes a $C-H\cdots O$ bond, and its signal shifts 1 ppm, whereas $H^{\epsilon 2}$ makes a $N-H\cdots O$ bond[26,27] and its δ_H shifts about 4 ppm. The validity of our complexes as reference to quantify SSHB effects on chemical shifts is reinforced by the fact that Westler et al. report for $H^{\delta 2}$ (atom not participating into hydrogen bonding) δ_H values of 7.26 (measured) and 6.89 ppm (calculated) in fair agreement with our result for that atom, 6.98 ppm (not shown in Figure 5).

These comparisons seem to imply that the large deshielding underlying the unusual downfield NMR chemical shifts observed in many biomolecular systems is mostly determined by the hydrogen bonding interaction itself. Not only the magnitude but, more important, the variations of δ_H in response to distance

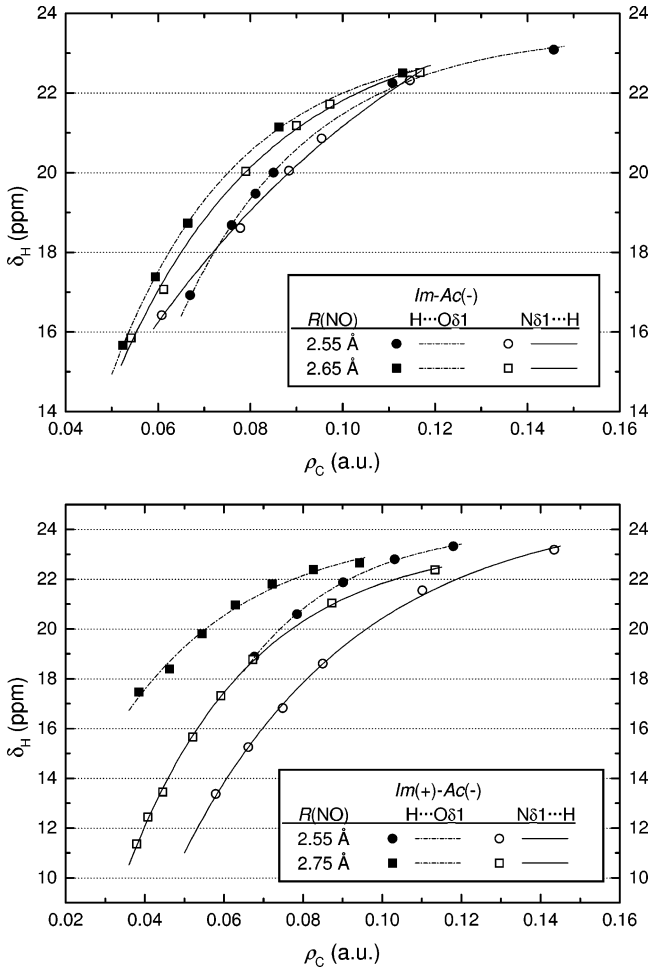

Figure 7. Dependence of B3LYP(ϵ = 1)/6-311++G(*d*,*p*) NMR chemical shifts on local values of the electron density at the hydrogen bond critical point, ρ_C, for the proton transferred from $N^{\delta1}$ to $O^{\delta1}$ in Im−Ac(−) (top panel) and Im(+)−Ac(−) (bottom panel). The curves are fits to eq 2.

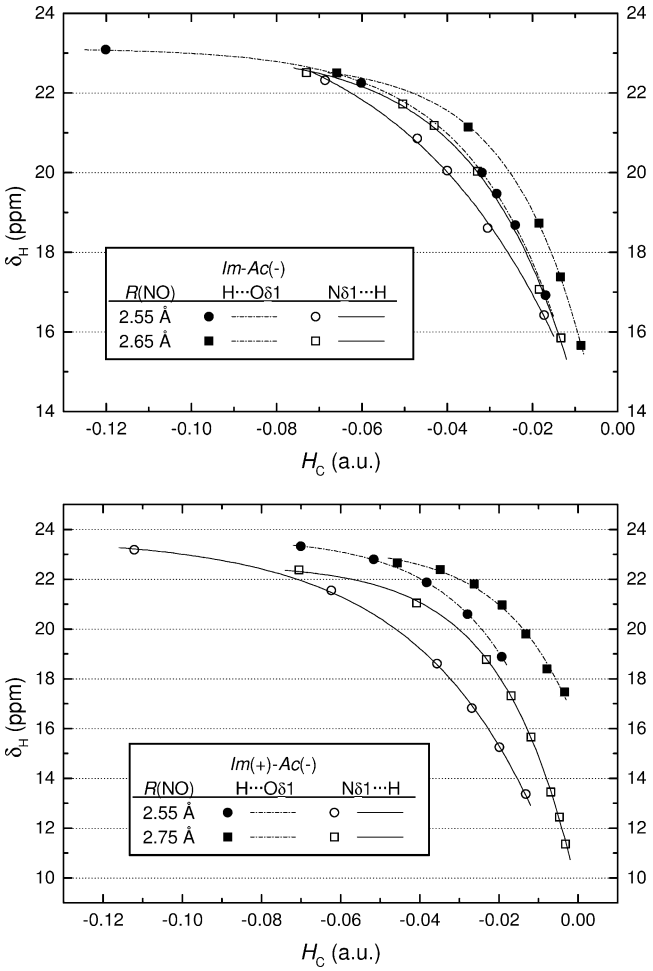

Figure 8. Dependence of B3LYP(ϵ = 1)/6-311++G(*d*,*p*) NMR chemical shifts on local values of the total energy density at the hydrogen bond critical point, H_C, for the proton transferred from $N^{\delta1}$ to $O^{\delta1}$ in Im−Ac(−) at *R*(NO) = 2.55 and 2.65 Å (top panel) and Im(+)−Ac(−) at *R*(NO) = 2.55 and 2.75 Å (bottom panel). The curves are fits to eq 3.

changes and protonation effects are reproduced to a great extent by the bare SSHB systems studied in this work. This agrees with previous reports demonstrating conclusively the lack of relationships between extremely low-field proton NMR signals and existence of LBHB.[8,18,19]

To assess the nature of hydrogen bonding effects on NMR chemical shifts, we turn now our attention to the electron density $\rho(\mathbf{r})$. The search of relationships between features associated with the strength of the interaction and a variety of topological descriptors of $\rho(\mathbf{r})$ has attracted great attention (the reader can find an updated account on this subject in refs 24 and 25). However, despite the direct influence of local electron density effects on chemical shifts, relationships between parameters derived from $\rho(\mathbf{r})$ and NMR data for HB systems have been much less investigated. In this regard, it is worth mentioning as an important exception the paper by Arnold and Oldfield[11] who related NMR $J_{NC'}$ couplings and proton chemical shifts measured in proteins with several AIM descriptors obtained from B3LYP $\rho(\mathbf{r})$ computed around selected N−H···O═C hydrogen bonds between backbone and side chains in available protein structures. While protein backbone HBs showed δ_H between 6.9 and 10.3 ppm, some SSHBs in enzyme/substrate complexes were found to exhibit chemical shifts between 12.4 and 21 ppm.[11]

A wealth of experience has lent support to properties locally computed at bond critical points (BCPs) of $\rho(\mathbf{r})$ as meaningful descriptors of the electron density. We focus here on two of such parameters that convey essential information on the nature of the interaction: the local values of the electron density, ρ_C, and the total energy density, H_C. As the proton moves from imidazole to acetate throughout $N^{\delta1}$−H···$O^{\delta1}$, $N^{\delta1}$···H···$O^{\delta1}$, and $N^{\delta1}$···H−$O^{\delta1}$ stages, bonds around the H atom change from covalent to hydrogen bonds. Figure 6 is a plot of the changes of ρ_C and H_C with R_{NH} for these complexes at equilibrium intermolecular distances. See in the top panel how ρ_C decreases smoothly from typical covalent values about 0.33 au at R_{NH} distances where the BCP belongs to either NH (open symbols) or HO (full symbols) covalent bonds, to about 0.05 au at the opposite side of the curves where the BCP belongs now to either N···H or H···O hydrogen bonds. This descriptor is the subject of one of the criteria proposed by Popelier et al. to characterize hydrogen bonding within AIM theory.[21] According to it, values of ρ_C within the range [0.002, 0.04] au [48] should be indicative of the existence of a HB, with greater values suggesting stronger interaction. As noticed in Figure 6, even the smallest values of ρ_C are still larger than 0.04 au in accordance with the SSHB nature of these systems. All the H_C curves plotted in the bottom panel are in the negative domain. Since the total energy density at a point is the sum of kinetic (always positive) and potential (always negative) energy densities, the resulting sign indicates which is the dominant contribution at the point.[21] As shown in

TABLE 2: Parameters in Equation 2 for the Hydrogen Bonds Involved in the Proton Transfer between $N^{\delta 1}$ and $O^{\delta 1}$ Atoms in the Complexes Displayed in Chart 1[a]

system	R(NO)	HB	domain of ρ_C	a_1	b_1	c_1	χ^2
Im−Ac(−)	2.55	H···O	0.065−0.148	23.56	70.52	35.20	0.021
	2.55	N···H	0.059−0.117	27.77	26.57	13.92	0.051
	2.65	H···O	0.050−0.115	23.35	52.28	36.54	0.0011
	2.65	N···H	0.052−0.119	23.80	42.44	30.61	0.088
Im(+)−Ac(−)	2.55	H···O	0.065−0.120	24.15	66.96	37.49	0.0043
	2.55	N···H	0.050−0.145	25.00	42.80	22.37	0.078
	2.75	H···O	0.036−0.096	24.06	22.00	30.53	0.033
	2.75	N···H	0.036−0.115	23.56	40.62	31.56	0.048

[a] R(NO) in Å; the rest of quantities in atomic units.

TABLE 3: Parameters in Equation 3 for the Hydrogen Bonds Involved in the Proton Transfer between $N^{\delta 1}$ and $O^{\delta 1}$ Atoms in the Complexes Displayed in Chart 1[a]

system	R(NO)	HB	domain of H_C	a_2	b_2	c_2	χ^2
Im−Ac(-)	2.55	H···O	−0.125 to −0.015	23.13	13.45	45.85	0.0018
	2.55	N···H	−0.072 to −0.015	24.47	12.71	26.18	0.036
	2.65	H···O	−0.068 to −0.008	22.76	11.51	56.50	0.0022
	2.65	N···H	−0.076 to −0.012	23.08	13.24	44.43	0.046
Im(+)−Ac(−)	2.55	H···O	−0.072 to −0.018	23.69	12.96	51.41	0.0010
	2.55	N···H	−0.116 to −0.012	23.68	15.71	31.47	0.025
	2.75	H···O	−0.048 to −0.003	23.33	7.333	53.71	0.085
	2.75	N···H	−0.074 to −0.002	22.61	13.23	56.87	0.036

[a] R(NO) in Å; the rest of quantities in atomic units.

AIM theory, the energy density dominant locally at a point is related with the sign of the Laplacian of $\rho(\mathbf{r})$ there, so when analyzing H_C, one is also including the information given by $\nabla^2\rho_C$.[20,21] Covalent bonds are characterized by large negative H_C values, whereas hydrogen bonds usually show small positive H_C, although, as it has been discussed elsewhere,[11,21,23−25] the presence of $H_C < 0$ in a HB critical point is interpreted as proof of strong interaction and hence the HB is assumed to have some degree of covalent character. The smooth transition between covalent and HB domains seen in Figure 6 without never reaching the $H_C > 0$ domain suggests a persistence of covalent character consistent with the strong nature of these HBs. It should be stressed that no distinction between covalent and hydrogen bonds is apparent: at intermediate distances where H is nearly equidistant from both heteroatoms, the interaction $N^{\delta 1}\cdots H\cdots O^{\delta 1}$ is neither purely covalent nor hydrogen bonding according to conventional standards. Incidentally, the apparent difference between complexes seen in the O···H → O−H curves is an artifact of taking the N−H instead of the O−H distance for plotting: had the independent variable been R_{OH}, the curves for Im−Ac(−) and Im(+)−Ac(−) should be also nearly indistinguishable.

As said above, Arnold and Oldfield found a relationship between NMR chemical shifts measured for protons participating in N−H···O═C hydrogen bonds in proteins and H_C computed using truncated geometries from crystal structures.[11] For a set of δ_H data between 7.3 and 21 ppm measured in free enzymes and enzyme/susbtrate complexes, they obtained H_C values ranging from +0.111 to −0.188 and showed that the relationship

$$H_C = a\exp(b\delta_H) - c \tag{1}$$

with $a = -6.1 \times 10^{-7}$, $b = 0.59$, and $c = 0.003$ (H_C in au, δ_H in ppm) reasonably holds for the sample although the range of large $\delta_H \sim 17-21$ ppm is the worst represented (see Figure 6 in ref 11). The rationale behind eq 1 is the already mentioned connection between stronger HBs and more deshielded protons, i.e., larger values of δ_H. Since both ρ_C and H_C descriptors reveal features of strong hydrogen bonding in our complexes, we searched for relationships such as that. To this end, we display in Figures 7 and 8 the dependence of B3LYP chemical shifts in the gas phase computed for the proton transferred on ρ_C and H_C, respectively. For every geometry considered, the $H\cdots O^{\delta 1}$ hydrogen bond corresponds to the range of δ_H less than or equal to its peak value, while $N^{\delta 1}\cdots H$ corresponds to δ_H values greater than this maximum. The curves plotted in these figures are fits to the relationship

$$\delta_H = a_1 - b_1\exp(-c_1\rho_C) \tag{2}$$

for the dependence on the electron density at the BCP and to

$$\delta_H = a_2 - b_2\exp(c_2H_C) \tag{3}$$

for the dependence on the total energy density at the BCP, being a_1, b_1, c_1, a_2, b_2, and c_2 fitted parameters whose values are collected in Tables 2 and 3. As the χ^2-values also listed in these tables demonstrate and it is readily apparent in Figures 7 and 8, the quality of the representations provided by eqs 2 and 3 is remarkable. Unlike the heterogeneous sample handled by Arnold and Oldfield, our data concern a single type of hydrogen bond, which allows focusing on effects underlying the interaction alone. The accurate representation provided by these exponential relationships confirms the close dependence of proton chemical shifts on characteristics obtained from the electron density at hydrogen bond critical points. Equation 2 concerns the dependence on the magnitude of the electron density itself: larger δ_H are associated with greater ρ_C values (see Figure 7) resulting from stronger HBs. Equation 3 concerns the dependence on the total energy density: larger δ_H are associated with more negative H_C that reveal increasingly greater partial covalent features. Summarizing, the extreme low-field NMR chemical shifts measured or computed for protons located farther from heteroatoms in strong HB systems are the direct consequence of local characteristics of the electron density distribution around H nuclei. Strong HBs formed upon the presence of charged monomers at close heteroatom distances accumulate electron density on hydrogen bond paths to a greater extent than conventional HBs. Consequently, the local dominant contribu-

tion of the potential energy density on HB paths increases, making the total energy density more negative, which indeed indicates that, as far as these descriptors are concerned, the underlying interaction is intermediate between covalent and hydrogen bonding. These local characteristics of the electron distribution around very deshielded protons may be viewed as the ultimate cause of the large NMR proton chemical shifts found in SSHBs.

Conclusions

The Im−Ac(−) and Im(+)−Ac(−) complexes at their equilibrium and one shorter heteroatom N···O distances have been selected to study the proton transfer from imidazole (either neutral in the former or protonated in the latter) to acetate. We have analyzed the influence of electron density effects on the variation of NMR proton chemical shifts δ_H along the H-transfer. The goal was to pose a model system to compare measured or computed δ_H data regarding biomolecular processes in which similar proton transfer under SSHB environments is known to play a leading role.

MP2/6-311++G(*d*,*p*) ab initio correlated calculations have been used to optimize geometries and compute electron densities, whereas NMR proton chemical shifts have been obtained at the B3LYP/6-311++G(*d*,*p*) level of theory. Electron correlation effects on δ_H are found to increase as the H atom places farther from heteroatoms; hence, it is absolutely mandatory to perform correlated calculations to obtain chemical shifts in proton transfers.

The comparison with computed values in the monomers reveals the very large deshielding suffered by the proton because of the strong nature of the HB. δ_H values are quite sensitive to the H heteroatom distance, but even at end stages of the transfer, low-field proton shifts in the 15−20 ppm range for N−H···O and 13−18 ppm for N···H−O localized states are found. Upon closer monomer approximation and consequently stronger hydrogen bonding, the proton NMR signal shifts even more downfield, especially in Im(+)−Ac(−). At delocalized N···H···O intermediate states the deshielding is maximum and δ_H reaches thus peak values about 23 ppm. All these results are in reasonable agreement with a host of data measured in SSHB dimers and active sites in free enzymes or enzyme/substrate complexes for which our bare systems are intended as reference to evaluate the magnitude of SSHB effects on NMR chemical shifts.

Finally, the dependence of δ_H on electron density properties computed along the H-transfer process has been also investigated. Exponential relationships between proton chemical shifts and two AIM topological descriptors usually employed to characterize the nature of interactions have been found to accurately represent the variations of δ_H. These descriptors are the local values at HB critical points of the electron density itself and the total energy density. They convey valuable information as far as their magnitudes allow, discussing the strength of the underlying interaction in terms of intermediate hydrogen bonding/covalent features. These relationships demonstrate that extreme low-field NMR chemical shifts observed in H-transfer under SSHB environments can be accurately quantified using local electron density characteristics that ultimately determine the great deshielding. Note finally that these large chemical shifts shown by delocalized protons in SSHB systems say nothing about the existence of LBHB.

Acknowledgment. The authors gratefully acknowledge financial support from Dirección General de Investigación, Ministerio de Ciencia y Tecnología of Spain, Project No. BQU2002-04005.

References and Notes

(1) Steiner, T. *Angew. Chem., Intl. Ed.* **2002**, *41*, 48.
(2) Perrin, C. L.; Nielson, J. B. *Annu. Rev. Phys. Chem.* **1997**, *48*, 511.
(3) (a) Gilli, P.; Bertolasi, V.; Ferretti, V.; Gilli, G. *J. Am. Chem. Soc.* **1994**, *116*, 909. (b) Dannenberg, J. J.; Paraskevas, L. R.; Sharma, V. *J. Phys. Chem. A* **2000**, *104*, 6617. (c) Grabowski, S. H.; Pogorzelska, M. *J. Mol. Struct.* **2001**, *559*, 201. (d) Humbel, S. *J. Phys. Chem. A* **2002**, *106*, 5517.
(4) Cleland, W. W.; Kreevoy, M. M. *Science* **1994**, *264*, 1887.
(5) For a review on LBHBs in enzymes see: (a) Cassidy, C. S.; Lin, J.; Frey, P. A. *Biochemistry* **1997**, *36*, 4576. (b) Cleland, W. W.; Frey, P. A.; Gerlt, J. A. *J. Biol. Chem.* **1998**, *273*, 25529. (c) Cleland, W. W. *Arch. Biochem. Biophys.* **2000**, *382*, 1. (d) Frey, P. A. *Magn. Reson. Chem.* **2001**, *39-S1*, S190.
(6) Schiott, B.; Iversen, B. B.; Madsen, G. K. H.; Larsen, F. K.; Bruice, T. C. *Proc. Natl. Acad. Sci. U.S.A.* **1998**, *95*, 12799.
(7) (a) Scheiner, S.; Kar, T. *J. Am. Chem. Soc.* **1995**, *117*, 6970. (b) Warshel, A. *J. Biol. Chem.* **1998**, *273*, 27035. (c) Schutz, C. N.; Warshel, A. *Proteins* **2004**, *55*, 711.
(8) Ash, E. L.; Sudmeier, J. L.; De Fabo, E. C.; Bachovchin, W. W. *Science* **1997**, *278*, 1128.
(9) Remer, L. C.; Jensen, J. H. *J. Phys. Chem. A* **2000**, *104*, 9266.
(10) Tuckerman, M. E.; Marx, D.; Klein, M. L.; Parrinello, M. *Science* **1997**, *275*, 817.
(11) Arnold, W. D.; Oldfield, E. *J. Am. Chem. Soc.* **2000**, *122*, 12835.
(12) Hibbert, F.; Emsley, J. *Adv. Phys. Org. Chem.* **1990**, *26*, 255.
(13) (a) Robillard, G.; Shulman, R. G. *J. Mol. Biol.* **1972**, *71*, 507. (b) Robillard, G.; Shulman, R. G. *J. Mol. Biol.* **1978**, *86*, 519.
(14) Mildvan, A. S.; Massiah, M. A.; Harris, T. K.; Marks, G. T.; Harrison, D. H. T.; Viragh, C.; Reddy, P. M.; Kovach, I. M. *J. Mol. Struct.* **2002**, *615*, 163.
(15) Frey, P. A. *J. Mol. Struct.* **2002**, *615*, 153.
(16) Stranzl, G. R.; Gruber, K.; Steinkellner, G.; Zangger, K.; Schwab, H.; Kratky, C. *J. Biol. Chem.* **2004**, *279*, 3699.
(17) Lin, J.; Westler, W. M.; Cleland, W. W.; Markley, J. L.; Frey, P. A. *Proc. Natl. Acad. Sci. U.S.A.* **1998**, *95*, 14664.
(18) García-Viloca, M.; Gelabert, R.; González-Lafont, A.; Moreno, M.; Lluch, J. M. *J. Phys. Chem. A* **1997**, *101*, 8727.
(19) Kumar, G. A.; McAllister, M. A. *J. Org. Chem.* **1998**, *63*, 6968.
(20) Bader, R. F. W. *Atoms in Molecules. A Quantum Theory*; Clarendon Press: Oxford, U.K., 1990.
(21) Popelier, P. *Atoms in Molecules. An Introduction*; Prentice Hall: Harlow, U.K., 2000.
(22) Gálvez, O.; Gómez, P. C.; Pacios, L. F. *Chem. Phys. Lett.* **2001**, *337*, 263.
(23) Gálvez, O.; Gómez, P. C.; Pacios, L. F. *J. Chem. Phys.* **2001**, *115*, 11166.
(24) Gálvez, O.; Gómez, P. C.; Pacios, L. F. *J. Chem. Phys.* **2003**, *118*, 4878.
(25) Pacios, L. F. *J. Phys. Chem. A* **2004**, *108*, 1187.
(26) Westler, W. M.; Weinhold, F.; Markley, J. L. *J. Am. Chem. Soc.* **2002**, *124*, 14373.
(27) (a) Molina, P. A.; Jensen, J. H. *J. Phys. Chem. B* **2003**, *107*, 6226. (b) Molina, P. A.; Sikorski, R. S.; Jensen, J. H. *Theor. Chem. Acc.* **2003**, *109*, 100.
(28) Shokhen, M.; Albeck, A. *Proteins* **2004**, *54*, 468.
(29) Rabuck, A. D.; Scuseria, G. E. *Theor. Chem. Acc.* **2000**, *104*, 439.
(30) Gómez, P. C.; Pacios, L. F. *Phys. Chem. Chem. Phys.*, submitted for publication.
(31) Biegler-Konig, F. W.; Bader, R. F. W.; Tang, T. H. *J. Comput. Chem.* **1982**, *3*, 317.
(32) (a) Ditchfield, R. *Mol. Phys.* **1974**, *27*, 789. (b) Dodds, J. L.; McWeeny, R.; Sadlej, A. J. *Mol. Phys.* **1980**, *41*, 1419. (c) Wolinski, K.; Hilton, J. F.; Pulay, P. *J. Am. Chem. Soc.* **1990**, *112*, 8251.
(33) Gilson, M. K.; Honig, B. H. *Biopolymers* **1986**, *25*, 2097.
(34) Schutz, C. N.; Warshel, A. *Proteins* **2001**, *44*, 400.
(35) (a) Miertus, S.; Scrocco, E.; Tomasi, J. *Chem. Phys.* **1981**, *55*, 117. (b) Mennucci, B.; Tomasi, J. *J. Chem. Phys.* **1997**, *106*, 5151. (c) Cammi, R.; Mennucci, B.; Tomasi, J. *J. Phys. Chem. A* **2000**, *104*, 5631. (d) Cossi, M.; Barone, V. *J. Chem. Phys.* **2001**, *115*, 4708. (e) Cossi, M.; Scalmani, G.; Rega, N.; Barone, V. *J. Chem. Phys.* **2002**, *117*, 43.
(36) Frisch, M. J.; Trucks, G. W.; Schlegel, H. B.; Scuseria, G. E.; Robb, M. A.; Cheeseman, J. R.; Zakrzewski, V. G.; Montgomery, J. A., Jr.; Stratmann, R. E.; Burant, J. C.; Dapprich, S.; Millam, J. M.; Daniels, A. D.; Kudin, K. N.; Strain, M. C.; Farkas, O.; Tomasi, J.; Barone, V.; Cossi, M.; Cammi, R.; Mennucci, B.; Pomelli, C.; Adamo, C.; Clifford, S.; Ochterski, J.; Petersson, G. A.; Ayala, P. Y.; Cui, Q.; Morokuma, K.; Malick, D. K.; Rabuck, A. D.; Raghavachari, K.; Foresman, J. B.; Cioslowski, J.;

Ortiz, J. V.; Baboul, A. G.; Stefanov, B. B.; Liu, G.; Liashenko, A.; Piskorz, P.; Komaromi, I.; Gomperts, R.; Martin, R. L.; Fox, D. J.; Keith, T.; Al-Laham, M. A.; Peng, C. Y.; Nanayakkara, A.; Gonzalez, C.; Challacombe, M.; Gill, P. M. W.; Johnson, B.; Chen, W.; Wong, M. W.; Andres, J. L.; Head-Gordon, M.; Replogle, E. S.; Pople, J. A. *GAUSSIAN98*, Revision A.7; Gaussian Inc.: Pittsburgh, PA, 1998.

(37) Frisch, M. J.; Trucks, G. W.; Schlegel, H. B.; Scuseria, G. E.; Robb, M. A.; Cheeseman, J. R.; Montgomery, J. A., Jr.; Vreven, T.; Kudin, K. D.; Burant, J. C.; Millam, J. M.; Iyengar, S. S.; Tomasi, J.; Barone, V.; Mennucci, B.; Cossi, M.; Scalmani, G.; Rega, N.; Petersson, G. A.; Nakatsuji, H.; Hada, M.; Ehara, M.; Toyota, K.; Fukuda, R.; Hasegawa, J.; Ishida, M.; Nakajima, T.; Honda, Y.; Kitao, O.; Nakai, H.; Klene, M.; Li, X.; Knox, J. E.; Hratchian, H. P.; Cross, J. B.; Adamo, C.; Jaramillo, J.; Gomperts, R.; Stratmann, R. E.; Yazyev, O.; Austin, A. J.; Cammi, R.; Pomelli, C.; Ochterski, J. W.; Ayala, P. Y.; Morokuma, K.; Voth, G. A.; Salvador, P.; Dannenberg, J. J.; Zakrzewski, V. G.; Dapprich, S.; Daniels, A. D.; Strain, M. C.; Farkas, O.; Malick, D. K.; Rabuck, A. D.; Raghavachari, K.; Foresman, J. B.; Ortiz, J. V.; Cui, Q.; Baboul, A. G.; Clifford, S.; Cioslowski, J.; Stefanov, B. B.; Liu, G.; Liashenko, A.; Piskorz, P.; Komaromi, I.; Martin, R. L.; Fox, D. J.; Keith, T.; Al-Laham, M. A.; Peng, C. Y.; Nanayakkara, A.; Challacombe, M.; Gill, P. M. W.; Johnson, B.; Chen, W.; Wong, M. W.; Gonzalez, C.; Pople, J. A. *GAUSSIAN03 (G03W)*, Revision B.02; Gaussian, Inc., Pittsburgh, PA, 2003.

(38) Foresman, J. B.; Keith, T. A.; Wiberg, K. B.; Snoonian, J.; Frisch, M. J. *J. Phys. Chem.* **1996**, *100*, 16098.

(39) Iwaoka, M.; Tomoda, S. *J. Comput. Chem.* **2003**, *24*, 1192.

(40) Wüthrich, K. *NMR of Proteins and Nucleic Acids*; Wiley: New York, 1986.

(41) Gross, K.; Kalbitzer, H. R. *J. Magn. Reson.* **1988**, *76*, 87.

(42) Chesnut, D. B. *Chem. Phys.* **1997**, *214*, 73.

(43) Barich, D. H.; Nicholas, J. B.; Haw, J. F. *J. Phys. Chem. A* **2001**, *105*, 4708.

(44) Bao, D. H.; Huskey, W. P.; Kettner, C. A.; Jordan, F. *J. Am. Chem. Soc.* **1999**, *121*, 4684.

(45) Bachovchin, W. W. *Magn. Reson. Chem.* **2001**, *39*, S199.

(46) Markley, J. L.; Westler, W. M. *Biochemistry* **1996**, *35*, 11092.

(47) Lin, J.; Cassidy, C. S.; Frey, P. A. *Biochemistry* **1998**, *37*, 11940.

(48) Koch, U.; Popelier, P. L. A. *J. Phys. Chem.* **1995**, *99*, 9747.